Colloid Polym Sci (2014) 292:863–871
DOI 10.1007/s00396-013-3127-2

ORIGINAL CONTRIBUTION

Inclusion complexes of α-cyclodextrins with poly(D,L-lactic acid): structural, characterization, and glass transition dynamics

Tânia Oliveira · Gabriela Botelho · Natália M. Alves · João F. Mano

Received: 18 July 2013 / Revised: 21 October 2013 / Accepted: 13 November 2013 / Published online: 3 December 2013

Abstract Poly (D,L-lactic acid) (PDLLA) was combined with α-CD to form inclusion complexes (ICs) with distinct PDLLA fractions. The structural changes resulting from this coalescence process were analyzed by Fourier transform infrared spectroscopy (FTIR), proton nuclear magnetic resonance (^{1}H NMR), and X-ray diffraction (XRD). The presence of both components in the ICs was confirmed by FTIR. The encapsulated PDLLA fraction was quantified by ^{1}H NMR. XRD data evidenced that it was possible to transform the amorphous PDLLA into a well-organized channel-type crystalline structure. DSC showed that the glass transition temperature of the PDLLA fraction in the ICs was higher than in the pure polymer, indicating that the ultra-confinement effect imposed by the ICs organization clearly limits PDLLA molecular dynamics. The confinement effect on the glass transition dynamics was investigated by unconventional dynamic mechanical analysis experiments, which confirmed that ICs segmental mobility is highly restricted when compared with the one of pure PDLLA. Bulk PDLLA presents a typical VFTH behavior while the ICs dynamics shows an Arrhenius trend.

T. Oliveira · N. M. Alves (✉) · J. F. Mano
3B's Research Group-Biomaterials, Biodegradables and Biomimetics, Engineering School, University of Minho, AvePark, Zona Industrial da Gandra, S. Cláudio do Barco, Caldas das Taipas, Guimarães 4806-909, Portugal
e-mail: nalves@dep.uminho.pt

T. Oliveira · N. M. Alves · J. F. Mano
ICVS/3B's PT Government Associate Laboratory, Braga, Guimarães, Portugal

G. Botelho
Chemistry Center, University of Minho, Campus de Gualtar, Braga 4710-057, Portugal

Keywords Poly(D,L-lactic acid) · Inclusion complexes · Glass transition dynamics

Introduction

A supramolecule is a system of two or more molecular entities held together and organized by means of inter-molecular non-covalent binding interaction [1, 2]. In this context, a variety of inclusion complexes (ICs) have been investigated, especially using cyclodextrins (CDs) as host molecules [3]. CDs result from the enzymatic degradation of starch. They are cyclic molecules containing six (α), seven (β), or eight (γ) glucose units joined by connections α-1,4-glycosidic linkages [4, 5]. These structures exhibit a truncated shallow cone shape with a hydrophobic cavity that is nonpolar in relation to the outer surface, suitable to act as a host for a variety of small guest molecules and to form ICs with distinct polymers. Regarding the ICs, the penetration of the macromolecular chains occurs inside of the CDs empty cavity and the rearrangement could lead to a well-organized structure [6, 7]. In this work, ICs were produced by combining CDs with the racemic copolymer of D-lactic acid and L-lactic acid, poly (D,L-lactic acid) (PDLLA): a biodegradable amorphous polyester, widely known and used in various biomedical applications, including as scaffolds for tissue engineering or in controlled drug release systems [8]. Most of the works regarding ICs of CDs and polymers are with semicrystalline polymers; an amorphous polymer such as PDLLA opens the very interesting possibility to produce an ordered structure from pure amorphous macromolecules.

ICs of PDLLA with α-CD were previously prepared [8, 9]. Another aim of this work was to increase the yield of the process by changing the previous experimental protocol [8, 9]. In fact, the quantity of obtained IC in the previous works was

extremely low when compared with the initial added amounts of PDLLA and α-CD.

The presence of PDLLA in the α-CD cavity was analyzed by: Fourier transform infrared spectroscopy (FTIR) and proton nuclear magnetic resonance (^{1}H NMR). The morphology of the different ICs was studied by scanning electron microscopy (SEM). X-ray diffraction (XRD) was used to investigate the organization of the IC structure.

The nanostructural IC organization is expected to restrict the geometrical confinement of the PDLLA chains. This geometrical holding would affect the glass transition dynamics due to the decrease of the molecular mobility. In fact, polymer chains in ICs are confined to occupy narrow channels (diameter ~0.5–1.0 nm) formed by the small-molecule hosts around the included guest polymers during IC self-assemble. The analysis of the confinement effect produced by an IC structure has not been properly addressed until now. Studies from our group [8, 9] and from Tonelli et al. [10] reported higher glass transition temperatures for polymers in ICs as compared to the bulk. The confinement of glass-forming systems has been analyzed in nanoporous glasses or zeolites [11, 12] or in ultra-thin films [13–15]. Another way of confining the glass-forming regions at the nanometer scale is by restricting the amorphous component of the macromolecules within the crystalline lamellae in semicrystalline polymers [16–20], which obviously influences the α-relaxation associated to the glass transition. Such studies of glass-forming systems in geometries of confining length at the nano-scale will allow a better understanding of the nature of the glass transition. This phenomenon is still far from being completely understood and constitutes a major issue in the field of soft condensed matter.

The confinement effect on the glass transition dynamics of PDLLA due to the IC structure was analyzed by differential scanning calorimetry (DSC) and dynamic mechanical analysis (DMA). The DMA experiments were performed in an unconventional way, using metallic pockets, in order to be able to characterize the glass transition dynamics of PDLLA and the ICs in a powder form.

Experimental section

The medical-grade PDLLA used in this work was obtained from Purac. The molecular weights of the polymer were M_n=31,750 and M_w=100,000 and used without further treatment and identified as "as-received" sample. α-CD was purchased from Fluka and used without further modification or treatment. 1,4-dioxane was obtained from Sigma-Aldrich.

The preparation of α-CD-PDLLA-IC was based on previous procedures [6, 8, 21]. However, in the present work, several changes were made to the preparation method of the inclusion complexes in order to optimize the overall process. To accelerate the dissolution of the PDLLA and α-CD samples, the dissolution temperature was raised to 60 °C. Therefore, the preparation time of α-CD and PDLLA solutions was significantly reduced from 1 day to 3 h and from 5 days to 3 days, respectively. The filtration was done with a glass Büchner funnel with pore diameter between 15–40 μm. By using this filtration methodology, ~2 g of α-CD-PDLLA-IC were collected, giving a yield of 52 wt% whereas in the method used in Ref. [5] the yield was 37 %. The protocol employed in this work permitted to reduce the time of synthesis of the ICs and decreased the loss of materials, as compared with previous methodologies [6, 8, 21]. Three ICs with distinct fractions of PDLLA were produced: IC1, IC2, and IC3. To obtain IC1, IC2, and IC3, 1.2, 3.2, and 6.4 g of PDLLA were respectively dissolved in 200 ml of dioxane, and heated at 60 °C during 3 days until complete dissolution of PDLLA. A 3.7-g sample of α-CD were dissolved in 25 ml of distilled water and heated during 3 h to accelerate α-CD dissolution. Then, the α-CD solution was slowly dipped into the PDLLA solution, while stirring. After adding all of the α-CD solution, the mixture was agitated for another hour at 60 °C. The heating was then stopped and the stirring was maintained overnight at room temperature. The resulting precipitate, a white powder, was filtered and washed several times either with dioxane or distilled water to remove non-complexed PDLLA and α-CD, respectively. Then, it was dried overnight under vacuum at room temperature.

PDLLA films were prepared by solvent casting using chloroform as solvent. After drying, films with about 150 μm thickness were obtained. The films were cut into rectangular strips to be used in the DMA tests. The PDLLA samples were also analyzed using metallic pockets.

PDLLA, α-CD and the ICs were characterized FTIR, using a Shimadzu-IR Prestige 21 FTIR spectrophotometer. The spectra were recorded in the wavenumber region between 400 and 4000 cm^{-1}. The number of scans was 35 and the resolution of 4 cm^{-1} with a % transmittance measurement mode and Happ–Genzel apodization.

The ^{1}H NMR analysis was performed on a Varian Unity Plus 300 MHz equipment. The acquisition of the spectra of PDLLA, α-CD and the ICs was performed at 25 °C using a delay (relaxation time) of 2 s and about 64 accumulations. The assignments were made with respect to the signal of dimethyl sulfoxide-d_6 (DMSO-d_6) at 2.5 ppm used as solvent for all samples.

The surface morphology of the developed ICs was analyzed using a Leica Cambridge S-360 scanning electron microscope (SEM). All samples were pre-coated with a conductive layer of sputtered gold. The analysis was performed at an accelerating voltage of 15 kV at different magnifications.

X-ray diffraction data were collected on a diffractometer X'Pert PRO-MPD (Philips/PANalytical), with a step (2θ=0.02°) scanning time of 2 s and Cu-Kα-radiation

generated at 40 kV and 30 mA. All XRD powder samples were obtained at ambient conditions.

DSC experiments were performed on a TA Q100 analyzer previously calibrated with indium and sapphire. Hermetically sealed aluminum pans were used in all experiments. The samples, with a weight of 8 mg, were previously aged for 70 h at 40 °C, after erasing the thermal history at 100 °C, in order to detect the glass transition more clearly. After the aging period, a first scan from 0 °C to 100 °C at 10 °C min^{-1} was performed The samples were then cooled immediately at 20 °C min^{-1} down to 0 °C and a second heating scan under the same conditions of the first heating scan was conducted. All DSC curves (PDLLA and the distinct ICs) were normalized using the total mass, i.e. 8 mg, as typically done to normalize DSC data of such supramolecular structures.

The viscoelastic measurements were performed using a TRITEC2000B dynamic mechanical analyzer from Triton Technology (UK), equipped with a single cantilever mode. The distance between the clamps was 15 mm and the samples were put inside pockets with 7.55 mm width. Temperature scans were performed by heating the samples at 0.1 °C/min from room temperature to 130 °C at several frequencies: 0.1, 0.2, 0.4, 2, 4, 10, 21, and 46 Hz. The experiments were performed under constant strain amplitude (50 μm). Both storage modulus (E') and loss factor (tan δ) were recorded as a function of temperature.

Results and discussion

As already explained in detail at the "Experimental section", several changes were made to the preparation method of the inclusion complexes in order to optimize the overall process, which permitted to reduce the time of synthesis of the ICs and decreased the loss of materials, as compared with previously employed methods [6, 8, 21].

FTIR analysis was conducted with the purpose of confirming the presence of PDLLA in the prepared ICs. Figure 1a shows the spectrum of PDLLA that are consistent with the ones found in literature [22–24]. The strong hydroxyl peak observed around 3,504 cm^{-1} is characteristics of the terminal hydroxyl –OH groups of PDLLA [25]. The peaks located at 3,000 cm^{-1} and 2,945 cm^{-1} are due to the stretching of the methyl groups (CH_3), together with the band at 1, 756 cm^{-1} due to carbonyl groups (C═O) [18, 23]. In the region from 1,380 to 1,453 cm^{-1} there are bands assigned to the methyl group and the band at 1,091 cm^{-1} is due to the C–O–C stretching [26, 27]. Among the characteristic bands of PDLLA, the one at 1,756 cm^{-1} is the most pronounced and, therefore, was used to analyze the inclusion of PDLLA in α-CD and it is shown an expanded view for a better understanding. When the FTIR spectra of the ICs, Fig. 1c, d, and e, are compared with the one of PDLLA, Fig. 1a, it is observed that all the ICs show this characteristic band, suggesting the effective formation of these ICs. Moreover, the intensity of this band is significantly higher for IC2 than for IC1, as expected, due to the increase of the percentage of PDLLA that was added to α-CD during the preparation of IC2. However, the intensity of this band does not undergo significant changes in IC3, despite the increase of the PDLLA percentage incorporated in this complex, when compared with IC2. These results suggested that the α-CD-PDLLA IC probably achieves a capacity limit, not allowing the incorporation of a higher amount of PDLLA than the one added in IC2.

The ICs, PDLLA and α-CD were analyzed by ^1H NMR to complement the FTIR data and further confirm and quantify the presence of PDLLA in the prepared complexes. These results are shown in Fig. 2.

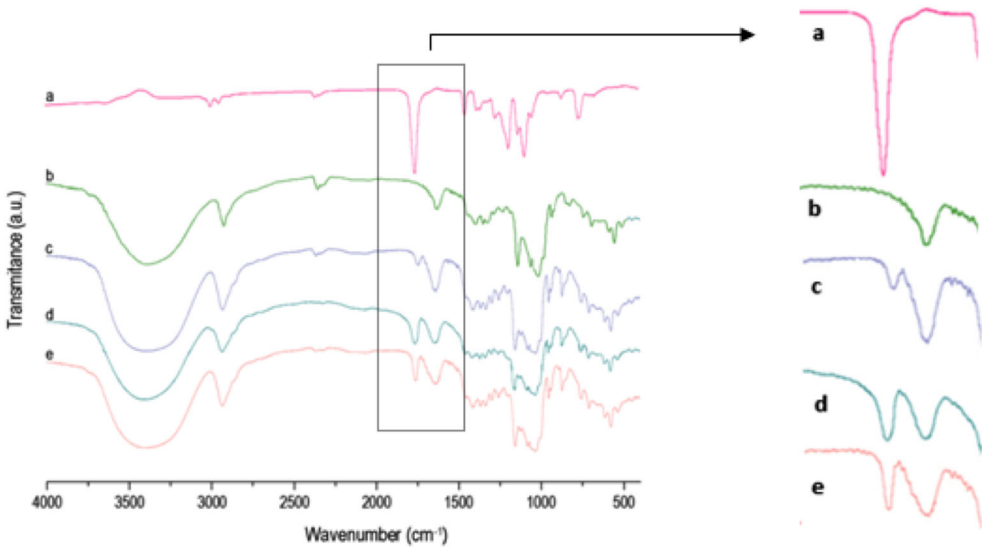

Fig. 1 FTIR spectra of PDLLA (**a**), α-CD (**b**), IC1 (**c**), IC2 (**d**) and IC3 (**e**). An expanded view at 1,756 cm^{-1} is included at the right side of the spectra

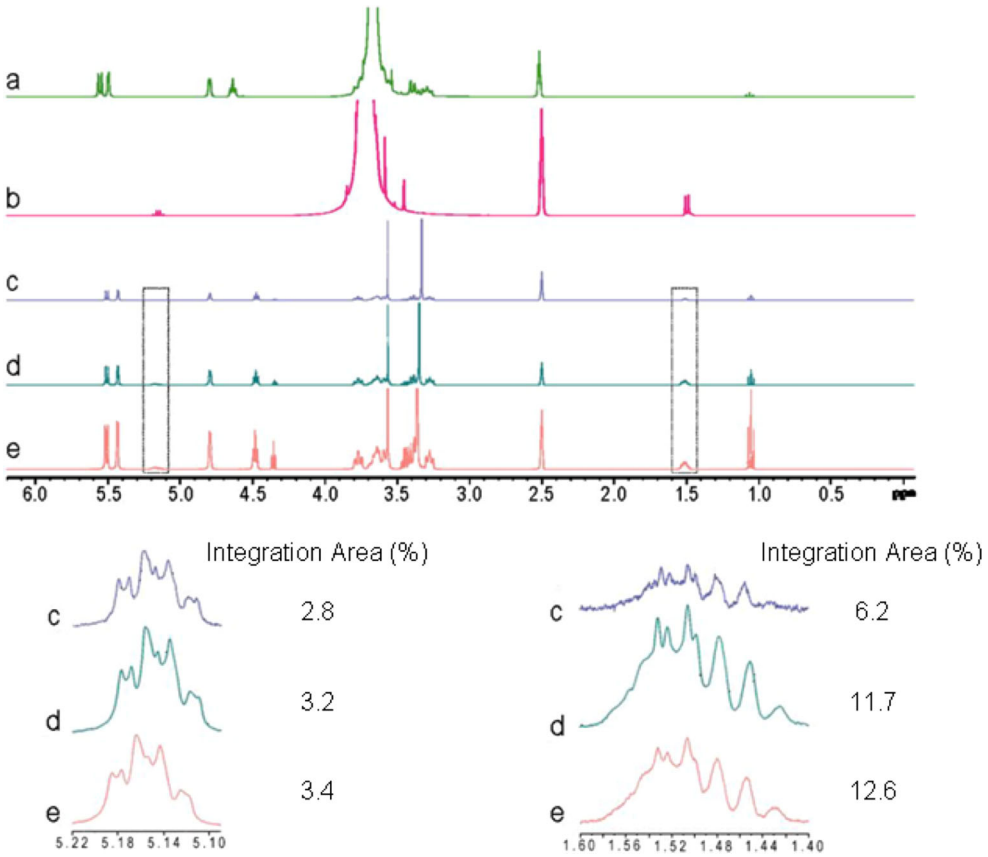

Fig. 2 ^{1}H NMR spectra of α-CD (**a**), PDLLA (**b**), IC 1 (**c**), IC 2 (**d**) and IC 3 (**e**) in DMSO-d_6. Below the ^{1}H NMR spectra it is shown the expanded view of the main multiplets with the respective integration area

The signal on the chemical shift of 2.49 ppm corresponds to the solvent, DMSO-d_6. Two main chemical shift (δ) values were obtained in the ^{1}H NMR spectra and were in agreement with the literature [28]. The multiplet at δ=1.54 ppm corresponds to the CH_3 protons attached to carbon. The intensity of the peaks shows that it is the order of 3 to 1 protons one being doublet. The multiplet at δ=5.18 ppm corresponds to the proton attached to carbon (CH) and is a quartet, indicating that it is surrounded by three protons.

^{1}H NMR also enabled to calculate the percentage of PDLLA incorporated in the three ICs taking into account the values of the integration area shown in Fig. 2. The values of PDLLA weight fraction initially added to α-CD and the ones incorporated can be found in Table 1. It can be seen that all ICs have the capacity to accommodate the polymer within the cavity of α-CD and that IC2 and IC3 presented a much higher fraction of PDLLA than IC1. However, although IC3 is the structure where the highest percentage of PDLLA was initially added to α-CD, the incorporated percentage is nearly the same as in IC2. This suggests that the supramolecular structure reaches its incorporation capacity limit.

Table 1 Weight percentage of PDLLA initially added (calculated based on the weights indicated at the experimental section) and incorporated (calculated based on the ^{1}H NMR results) in the supramolecular structure of the different ICs

	IC1 (%)	IC2 (%)	IC3 (%)
PDLLA initial	24	46	63
PDLLA incorporated	10	15	16

Data of α-CD resonance shift to all protons, in the presence of PDLLA, are shown in Table 2. According to the literature [29, 30], the protons of the cavity of α-CD, H-3 and H-5 should show changes in the resonance signals in the presence of the molecule that is being incorporated. On the other hand, the remaining hydrogens belonging to the outer cavity will not likely show large changes in signals. In our case, the signals of α-CD showed significant changes in the presence of PDLLA. The protons located within the cavity of α-CD, namely H-3 and H-5, showed significant changes in chemical shifts (upfield), typical of the presence of inclusion, while the protons located on the outside (H-1, H-2, and H-4) showed insignificant changes of downfield frequency. However, the signal related to the H-2 shows a slightly more significant change than H-1 and H-4. This may possibly be due to some polymer residue present outside the structure after washing with dioxane that was carried out and described in the experimental part [29]. The upfield frequency shift of the H-3 and H-6 protons and downfield shift of H-5 in the α-CD cavity suggests its involvement in hydrophobic interactions as an unambiguous indicator of the interaction of PDLLA with the

Table 2 ^{1}H NMR chemical shifts of α-CD, free and after complexation with PDLLA [28]

Proton	δ_{free} (ppm)	δ_{bound} (ppm) IC1	δ_{bound} (ppm) IC2	δ_{bound} (ppm) IC3	$\Delta\delta=\delta_{bound}-\delta_{free}$ (ppm) IC1	$\Delta\delta=\delta_{bound}-\delta_{free}$ (ppm) IC2	$\Delta\delta=\delta_{bound}-\delta_{free}$ (ppm) IC3
H-1	5.49	5.49	5.49	5.49	0.00	0.00	0.00
H-2	3.36	3.35	3.35	3.35	−0.01	−0.01	−0.01
H-3	3.65	3.64	3.62	3.63	−0.01	−0.03	−0.02
H-4	3.26	3.26	3.26	3.26	0.00	0.00	0.00
H-5	3.37	3.38	3.38	3.38	+0.01	+0.01	+0.01
CH_2-6	3.40	3.39	3.39	3.39	−0.01	−0.01	−0.01

interior of the α-CD cavity resulting in the formation of the inclusion complex PDLLA-α-CD-IC [30].

The analysis of the surface of the developed ICs was performed by SEM—see Fig. 3. These images suggest the formation of microstructures with sizes between 1 and 2 μm, with irregular geometry. Moreover, it can also be noted that, as the percentage of PDLLA increases from IC1 to IC3, the structures tend to become larger.

The organization of the structure of the complexes was analyzed by XRD. X-ray diffractograms of pure α-CD and IC2 are shown in Fig. 4a. X-ray diffractograms of IC1 and IC3 are similar to the one corresponding to IC2 (data not shown). The XRD pattern of α-CD shows intense and sharp peaks that confirmed the crystalline nature of the compound, PDLLA is an amorphous material and therefore presents no crystalline peaks (data not shown). On the other hand, the IC is a very well-organized material. The peaks detected at $2\theta=7.56$, 13.12, and 19.9—seen in Fig. 4a (II) are very similar to those observed in an IC of α-CD with poly(ε-caprolactone) [31, 32]. The inclusion of PDLLA in the cavity of pure α-CD causes a rearrangement which generates a new crystalline structure. The peak at $2\theta=19.9°$—seen in Fig. 4a (II)—proves the intimate change at the lattice level during inter-penetration of CD with PDLLA [31, 33].

During the preparation of the inclusion complexes, a channel-type structure was probably developed, which is consistent with the strong diffraction peak found at around $2\theta=19.9°$ [6]. In this organization, the polymer chains are included in a well-organized structure of α-CD molecules [6, 31]—see scheme in Fig. 4b.

Thus, from the ^{1}H NMR and XRD results, it can be said that the α-CDs are closely packed along the PDLLA chain and the single IC strands are aligned in the horizontal direction, as depicted in the scheme of Fig. 4b. The α-CD rings are stacked one over the other in order to produce core cylindrical cavities through which the polymer chains pass.

The strong confinement of the PDLLA chains in IC structure should have consequences in the molecular dynamics of the polymer. In semicrystalline polymers, the conformational mobility of the chains of the amorphous phase is significantly limited near the crystalline phase. This typically leads to an increase in T_g, when compared with the T_g of the same polymer in the amorphous state and to a broadening of the glass transition [16, 34]. Regarding the glass transition of glass-forming materials confined in nanopores, where positive, negative or negligible T_g shifts have been observed, it has been suggested that there is an intrinsic size effect and that the confinement effects are also due to the details of the interactions between the surface of the confining medium and the confined liquid or polymer [13, 35]. For thin polymer films, there is evidence that the interaction between the substrate and the film and the method of film preparation can play a crucial role in determining the sign of the shift in T_g, that can also be positive, negative or negligible [13, 36].

In this work, the dynamics of the glass transition of PDLLA and the distinct ICs was analyzed by DSC. Figure 5 shows the DSC results obtained with the samples previously subjected to an aging period of 70 h at 40 °C.

For the case of PDLLA (Fig. 5a), the presence of an endothermic peak of high magnitude associated to the

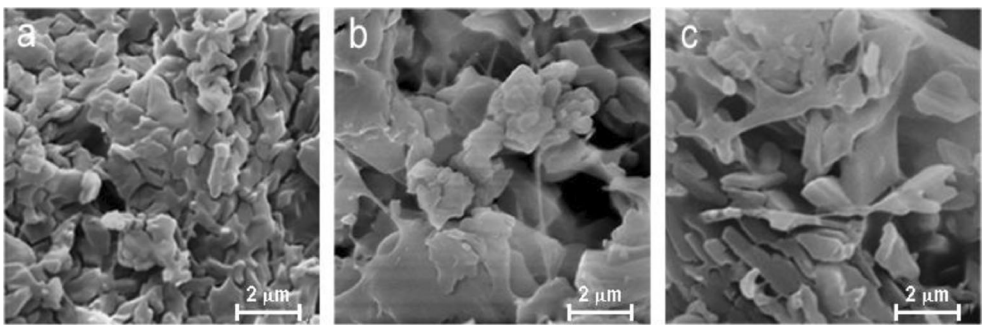

Fig. 3 SEM images of surface structure of IC1 (**a**), IC2 (**b**) and IC3 (**c**)

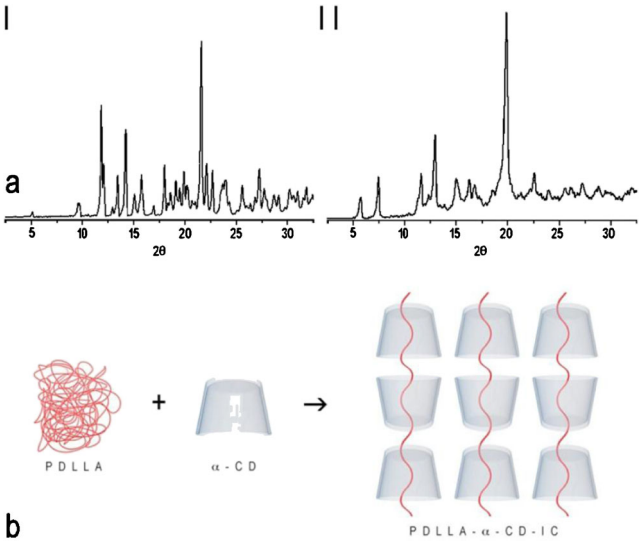

Fig. 4 **a** X-ray diffraction pattern of α-CD (*I*) and IC 2 (*II*); **b** schematic structure of the IC obtained by combining α-CD and PDLLA

enthalpy recovery of the material that was previously subjected to a physical aging process, is clearly seen. The second scan shows the presence of a glass transition at nearly 50 °C. The T_g is detected by the typical step change in the heat flow curve [18, 37]. For IC2 and IC3 (Fig. 5c, d) the endothermic peak was also detected under the same aging conditions, both showing the same amplitude, but much lower when compared to the one corresponding to PDLLA. For IC1 (Fig. 5b), this peak was not even detected due to the low amount of PDLLA present in this sample when compared with IC2 and IC3. The second scans of IC2 and IC3 show the presence of a T_g at nearly 56 °C, being also the step change in the heat flow due to the glass transition process less intense than the one corresponding to PDLLA, as expected. The T_g increase can be explained by the restricted chain mobility of the PDLLA chains in the ICs. A jump in C_p analogous to a glass transition implies a change in the temperature dependence of the number of microstates Ω available for the polymeric chains, as deduced from Boltzmann's equation $S = k \ln \Omega$ and $C_p = T(dS/dT) = kT(d\ln\Omega/dT)$ where S is the entropy and k is the Boltzmann constant [38]. This occurs during the glass transition in amorphous systems because of the exponential increase of the number of configurational states with increasing temperature in the liquid state. Any segmental mobility that takes place in the IC does not involve such significant variations in the number of microstates, and thus the heat capacity is not expected to experience a considerable variation [9], as occurs in this work.

By looking at Fig. 5, it can also be seen that for the ICs the approximate value of the heat capacity step at T_g is around 0.3 J/K g (Fig. 5b, c, d—second runs). This value is very low when compared with the values for PDLLA, which is around 0.8 J/g K, as found in this work (Fig. 5a—second run) and also in [9]. The negligible heat capacity change of the ICs is also a consequence of the strong confinement effect imposed by the IC structure on the glass transition dynamics, limiting the mobility of the polymeric chains in the channel structure of the IC.

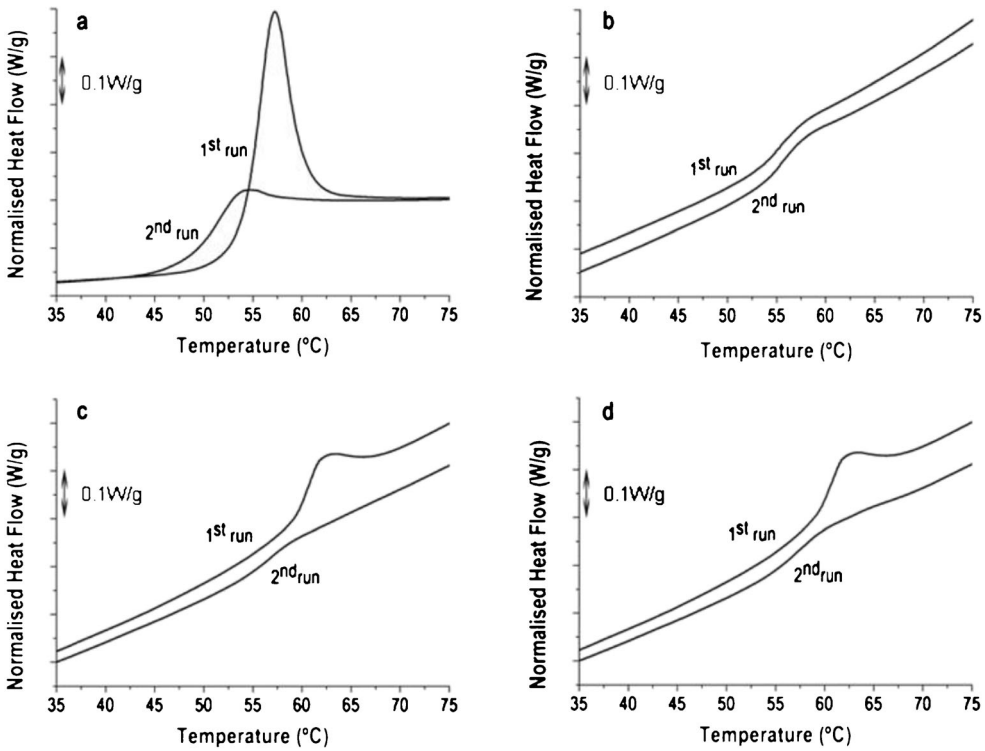

Fig. 5 DSC scans of PDLLA (**a**), IC1 (**b**), IC2 (**c**) and IC3 (**d**) after an aging period at 40 °C for 70 h

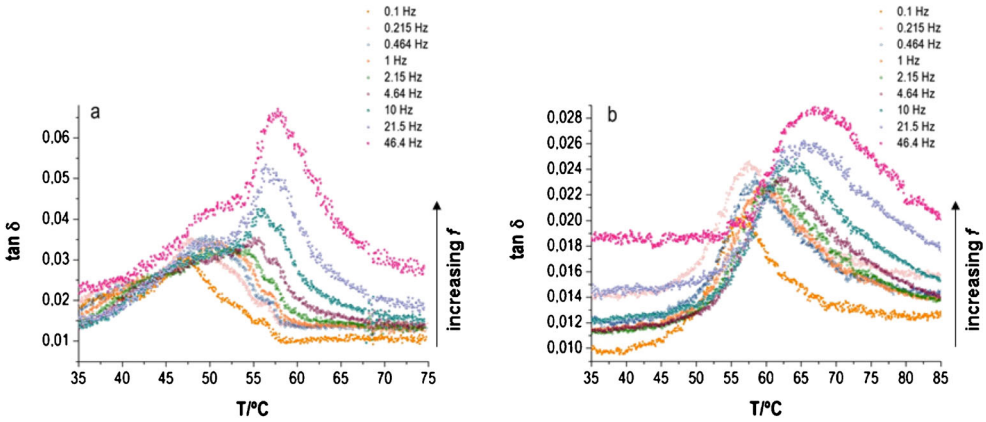

Fig. 6 Loss factor at different frequencies for a PDLLA film (**a**) and IC2 powder (**b**) placed in metallic pockets

It should be pointed that only the glass transition region of the ICs and pure PDLLA was shown in the data of Fig. 5, because it was the region that we intended to analyze and also because above the glass transition we didn't observe any melting, as expected, because pure PDLLA is an amorphous polymer. Polylactides in the amorphous state present a typical amorphous XRD pattern, indicating the absence of melting [39]. On the other hand, there are several previous works that reported the DSC data of pure α-CD and inclusion complexes (ICs) based on α-CD and distinct semicrystalline polymers [2, 31, 32, 40]. These works evidenced that α-CD and typically their ICs do not show any detectable thermal transitions in the heating scans, namely melting, and this happens because they decompose while melting. In this case, the absence of the melting peak corresponding to the pure semicrystalline polymer indicates that the crystallization of the guest polymer is suppressed because all the semicrystalline polymeric chains are included and isolated in the CD channels. In some cases, a melting peak with a much lower intensity than the one of the pure polymer can be detected, which indicates the presence of some crystallizable polymer chains outside the CD cavity [32].

The glass transition dynamics of the ICs was analyzed in more detail by DMA. A great advantage of DMA is the ability to analyze the glass transition dynamics at different frequencies and, hence, in a broader time scale than DSC. Based on the previous results, it is evident that IC2 was the complex that combines the best features for further analysis of the relaxational behavior in the glass transition region.

DMA tests were performed on both PDLLA and IC2 using an unconventional metallic pocket method because it permits study IC2 in a powder form. The loss factor variations as a function of temperature for the chosen frequencies are shown in Fig. 6. The α-relaxation peaks are well resolved and the temperatures of the maxima are easily detected. A clear shift towards higher temperatures is observed for the tan δ peaks with increasing frequency for both materials.

For IC2, the maximum of the α-relaxation peak appears at around 60 °C at the frequency of 1 Hz, whereas for PDLLA this maximum occurred at 50 °C. The temperature of tan δ maximum is a measure of the T_g of the material. These results evidenced that the T_g of the IC increased 10 °C, when compared with the one of PDLLA. This should be a consequence of the confinement effect resulting from the organization at the nano-scale level in the IC, limiting the conformational mobility of the PDLLA chains, in agreement with the DSC results. Another effect of the confinement is the broadening of the loss factor peaks of the IC when compared with the ones of PDLLA. These effects are similar to what happens in distinct semicrystalline polymers and in particular in PLLA [16, 34, 41] and PET [42]. For example, PLLA samples were prepared with different degrees of crystallinity and subjected to aging [37]. For intermediate crystallinities two endothermic peaks assigned to enthalpy recovery were detected by DSC, indicating the existence of two distinct glass transition dynamics. The low-temperature process was assigned to the bulk-like glass transition whereas the broader high-temperature process was attributed to the restricted motions of the amorphous phase confined by the crystalline structures. It was suggested that the effect of confinement exerted by crystalline phase should be mainly dominated by the nature of the interface between the free amorphous phase and the rigid phase and not due to the

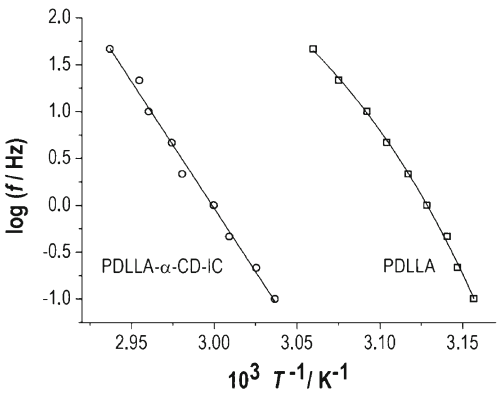

Fig. 7 Relaxation map for PDLLA (*squares*) and IC2 (*circles*), obtained from the data shown in Fig. 6, with the corresponding VFTH and Arrhenius fits, respectively (*solid lines*)

geometrical confinement itself. For comparison, note that the confinement effect produced by the crystalline lamellae in semicrystalline PLLA leads to an increase in T_g of between 4 and 8 °C, depending on the crystalline degree [8, 43]. For the semicrystalline case the mobile amorphous phase is confined between the crystalline lamellae and for the case of the ICs, the PDLLA chains adopt a much more aligned configuration, where they must pass through the cavities of the α-CDs which are also organized in a supramolecular structure. Therefore, the confinement effect found in the IC is highly superior to the one that has been found in semicrystalline polymers [1]. The effect of confinement on the glass transition dynamics of PDLA and PLLA thin films has also been analyzed [44]. In that study, the initial organization of macromolecules within the film or the configuration of the enantiomeric chains did not yield any variation in T_g. This non-deviation of T_g in respect with the bulk polymer was attributed to the balance between the strength of the interfacial interactions and the decrease in PLA crystallinity in thin films.

The maximum tan δ temperatures as a function of frequency for both PDLLA and IC2 were collected in a relaxation plot—see Fig. 7.

For PDLLA, a clear curvature was found. These results were fitted according to the Vogel–Fulcher–Tamman–Hesse equation (VFTH):

$$\tau(\mathrm{T}) = \tau_0 \exp\left(\frac{\mathrm{B}}{\mathrm{T}-\mathrm{T}_0}\right)$$

where τ_0 is a pre-exponential factor and B and T_0 are specific adjustable material parameters. The values of $\tau(T)$ were obtained from the frequency of the experiments: $\tau = 1/(2\pi f)$. The best fit yielded the following adjustable parameters: $\ln \tau_0$ (s)=−18.5 ±6.8; B=640±44 K and T_0=285.8±10.7 K (R^2=0.992)—see solid line in Fig. 7. The VFTH behavior was not found in the relaxation plot of the IC, which exhibited a more linear relationship. Such trend suggests that the IC behaves as a "strong" system, according to the fragile/strong classification proposed by Angell [9] whereas the amorphous PDLLA exhibits a more fragile nature. Assuming an Arrhenius dependency for the IC, where $\ln \tau \propto \mathrm{E_a}/(RT)$, being E_a the activation energy and R is the ideal gas constant, a value of E_a=488±38 kJ mol^{-1} (R^2=0.985) was obtained by linear regression. Such a value is higher than the activation energies observed for the glass transition of semicrystalline PLLA obtained using mechanical spectroscopies, which were typically lower than 400 kJ mol^{-1} [9]. Hence, it can be said that the confinement effect exerted by the organized arrangement at the sub-nanometer level in the IC leads to different glass transition dynamics than that found in the bulk state or even in semicrystalline systems. It is interesting to note that Zuza et al. showed that amorphous PDLLA is a stronger glass former than semicrystalline PLLA [16]. This means that crystallinity and the presence of a rigid amorphous phase not only elevate T_g but also increase the dynamic fragility of polylactide chains around the T_g. The T_g value can also be estimated from the resulting parameters in both equations. A T_g of nearly 40 °C was obtained for PDLLA, whereas a T_g of nearly 50 °C was obtained for the IC. Although these values are somewhat lower than the ones obtained by DSC and DMA at 1 Hz (Figs. 5 and 6), a T_g increase of about 10 °C was obtained for the IC in agreement with both DSC and DMA data.

The results found in this work also demonstrate that DMA data obtained using metallic pockets have great potential to extract information about the effect of confinement on the glass transition dynamics of materials where the glass transition could not be measured by conventional DMA tests.

Conclusion

An improved methodology was employed to produce PDLLA-α-CD-ICs. A series of techniques demonstrated the presence of PDLLA in the supramolecular structure. ^{1}H NMR data confirmed the coalescence of PDLLA in this structure through the hydrophobic cavity interactions. XRD measurements demonstrated that through the combination of the amorphous polymer with cyclodextrins, a material with a well-organized arrangement was obtained adopting a crystalline channel-type organization. The dynamics of the glass transition of both materials was investigated by DSC and through DMA using a metallic pocket methodology. This showed that the T_g of bulk PDLLA lies at lower temperatures when compared with the T_g of the ICs, which demonstrates the high effect of confinement imposed by the α-CD rings that restricts the conformational dynamics of the PDLLA chains.

Acknowledgments Portuguese Foundation for Science and Technology (FCT) for financial support through the PTDC/FIS/115048/2009 project and to the NMR Portuguese network (PTNMR, Bruker Avance III 400-Univ. Minho). FCT and FEDER (European Fund for Regional Development)-COMPETE-QREN-EU for financial support to the Research Centre, CQ/UM [PEst-C/QUI/UI0686/2011 (FCOMP-01-0124-FEDER-022716)].

References

1. Jeong S, Kang WY, Song CK, Park JS (2012) Supramolecular cyclodextrin–dye complex exhibiting selective and efficient quenching by lead ions. Dyes Pigments 93:1544–1548
2. Wang L, Wang JL, Dong CM (2005) Supramolecular inclusion complexes of star-shaped poly(ε-caprolactone) with α-cyclodextrin. J Polym Sci A Polym Chem 43:4721–4730
3. Ceborska M, Asztemborska M, Lipkowski J (2012) Rare 'head-to-tail' arrangement of guest molecules in the inclusion complexes of (+)- and (−)-menthol with β-cyclodextrin. Chem Phys Lett 553:64–67
4. Celebioglu A, Uyar T (2011) Electrospinning of polymer-free nanofibers from cyclodextrin inclusion complexes. Langmuir 27:6218–6226

5. Castiglione F, Crupi V, Majolino D, Mele A, Rossi B, Trotta F et al (2012) Inside new materials: an experimental numerical approach for the structural elucidation of nanoporous cross-linked polymers. J Phys Chem B 116:13133–13140
6. Williamson BR, Krishnaswamy R, Tonelli AE (2011) Physical properties of poly(ε-caprolactone) coalesced from its α-cyclodextrin inclusion compound. Polymer 52:4517–4527
7. Zhang S, Yu Z, Govender T, Luo H, Li B (2008) A novel supramolecular shape memory material based on partial α-CD–PEG inclusion complex. Polymer 49:3205–3210
8. Pinheiro A, Mano JF (2009) Study of the glass transition on viscous-forming and powder materials using dynamic mechanical analysis. Polym Test 28:89–95
9. Mano JF (2008) Thermal behaviour and glass transition dynamics of inclusion complexes of α-cyclodextrin with poly(D,L-lactic acid). Macromol Rapid Commun 29:1341–1345
10. Tonelli AE (2012) Superstructures with cyclodextrins: chemistry and applications. Beilstein J Org Chem 8:1318–1332
11. Richert R (2011) Dynamics of nanoconfined supercooled liquids. Annu Rev Phys Chem 62:65–84
12. Korotkova T, Karaeva O, Naberezhnov A, Rysiakiewichz-Pasek E, Korotkov L (2012) Dielectric and mechanical relaxations in the vicinity of glass transitions in confined polar copolymers VDF/Te and VDF/Tr. Solid State Commun 152:846–848
13. Richert R (2011) Dynamics of nanoconfined supercooled liquids. Annu Rev Phys Chem 62:65–84
14. McKenna GB (2010) Ten (or more) years of dynamics in confinement: perspectives for 2010. Eur Phys J Spec Top 189:285–302
15. Modestino MA, Paul DK, Dishari S, Petrina SA, Allen FI, Hickner MA et al (2013) Self-assembly and transport limitations in confined Nafion films. Macromolecules 46:867–873
16. Zuza E, Ugartemendia JM, Lopez A, Meaurio E, Lejardi A, Sarasua JR (2008) Glass transition behavior and dynamic fragility in polylactides containing mobile and rigid amorphous fractions. Polymer 49:4427–4432
17. Wang Y, Gómez Ribelles JL, Salmerón Sánchez M, Mano JF (2005) Morphological contributions to glass transition in poly(L-lactic acid). Macromolecules 38:4712–4718
18. Delpouve N, Lixon C, Saiter A et al (2009) Amorphous phase dynamics at the glass transition in drawn semi-crystalline polyester. J Therm Anal Calorim 97:541–546
19. Delpouve N, Saiter A, Dargent E (2011) Cooperativity length evolution during crystallization of poly(lactic acid). Eur Polym J 47:2414–2423
20. Hamonic F, Saiter A, Prevosto D et al (2012) Temperature dependence of structural relaxation time in drawn polymers: which is the role of cooperativity? AIP Conf Proc 1459:211–213
21. Chen C-C, Chueh J-Y, Tseng H, Huang H-M, Lee S-Y (2003) Preparation and characterization of biodegradable PLA polymeric blends. Biomaterials 24:1167–1173
22. Kister G, Cassanas G, Vert M (1998) Effects of morphology, conformation and configuration on the IR and Raman spectra of various poly (lactic acid). Polymer 39:267–273
23. Matusik J, Stodolak E, Bahranowski K (2011) Synthesis of polylactide/clay composites using structurally different kaolinites and kaolinite nanotubes. Appl Clay Sci 51:102–109
24. Meaurio E, Lopez-Rodriguez N, Sarasua J (2006) Infrared spectrum of poly (L-lactide): application to crystallinity studies. Macromolecules 39:9291–9301
25. Tonelli AE (2012) Restructuring polymers via nanoconfinement and subsequent release. Beilstein J Org Chem 8:1318–1332
26. Dias JCR. Desenvolvimento de um fio de sutura degradável baseado em PLLA com libertação controlada de fármacos. Master Thesis, Universidade do Minho, Portugal, 2011
27. Correia C, Moreira Teixeira LS, Moroni L, Reis RL, van Blitterswijk C, Karperien M et al (2011) Chitosan scaffolds containing hyaluronic acid for cartilage tissue engineering. Tissue Eng Part C 17:717–730
28. Liu X, Zou Y, Li W, Cao G, Chen W (2006) Kinetics of thermo-oxidative and thermal degradation of poly(D,L-lactide) (PDLLA) at processing temperature. Polym Degrad Stab 91:3259–3265
29. Faucci MT, Melani F, Mura P (2000) 1H-NMR and molecular modelling techniques for the investigation of the inclusion complex of econazole with α-cyclodextrin in the presence of malic acid. J Pharm Biomed Anal 23:25–31
30. Anselmi C, Centini M, Maggiore M, Gaggelli N, Andreassi M, Buonocore A et al (2008) Non-covalent inclusion of ferulic acid with α-cyclodextrin improves photo-stability and delivery: NMR and modeling studies. J Pharm Biomed Anal 46:645–652
31. Huang L, Allen E, Tonelli AE (1998) Study of the inclusion compounds formed between α-cyclodextrin and high molecular weight poly(ethylene oxide) and poly(ε-caprolactone). Polymer 39:4857–4865
32. Mori T, Dong T, Yazawa K, Inoue Y (2007) Preparation of highly transparent and thermally stable films of α-cyclodextrin/polymer inclusion complexes. Macromol Rapid Commun 28:2095–2099
33. Wenz G, Han B-H, Mueller A (2006) Cyclodextrin rotaxanes and polyrotaxanes. Chem Rev 106:782–817
34. Wang Y, Gómez Ribelles JL, Salmerón Sánchez M, Mano JF (2005) Morphological contributions to glass transition in poly(L-lactic acid). Macromolecules 38:4712–4718
35. McKenna GB (2005) Effects of confinement on material behaviour at the nanometre size scale. J Phys Condens Matter 17:R261–R524
36. Eastman SA, Kim S, Page KA, Rowe BW, Kang S, Soles CL et al (2012) Effect of confinement on structure, water solubility, and water transport in Nafion thin films. Macromolecules 45:7920–7930
37. Mano JF, Gómez Ribelles JL, Alves NM, Salmerón Sanchez M (2005) Glass transition dynamics and structural relaxation of PLLA studied by DSC: influence of crystallinity. Polymer 46:8258–8265
38. Wool RP, Campanella A (2009) Twinkling fractal theory of the glass transition: rate dependence and time–temperature superposition. J Polym Sci Part B Polym Phys 47:2578–2590
39. Mano JF (2007) Structural evolution of the amorphous phase during crystallization of poly(L-lactic acid): A synchrotron wide-angle X-ray scattering study. J Non-Cryst Solids 353:2567–2572
40. Huh KM, Cho YW, Chung H, Kwon IC, Jeong SY, Ooya T, Lee WK, Sasaki S, Yui N (2004) Supramolecular hydrogel formation based on inclusion complexation between poly(ethylene glycol)-modified chitosan and α-cyclodextrin. Macromol Biosci 4:92–99
41. Dionisio M, Viciosa MT, Wang Y, Mano JF (2005) Macromol Rapid Commun 26:1423
42. Lixon C, Delpouve N, Saiter A et al (2008) Evidence of cooperative rearranging region size anisotropy for drawn PET. Eur Polym J 44: 3377–3384
43. Delpouve N, Saiter A, Mano JF et al (2008) Cooperative rearranging region size in semi-crystalline poly(L-lactic acid). Polymer 49: 3130–3135
44. Narladkar A, Balnois E, Vignaud G, Grohens Y (2008) Difference in glass transition behavior between semi crystalline and amorphous poly(lactic acid) thin films. Macromol Symp 273:146–152